Sensors and Materials, Vol. 38, No. 7 (2026) 4125–4140
MYU Tokyo

S & M 4554

Sensor-based Digital Twins: Perceptual and Spatial Evaluation by Comparing Physical and Virtual Reality Exhibitions

Ming Zhang[1] and Hsin-Hung Lin[1,2*]

[1]Institute of Creative Arts and Design, UCSI University, Kuala Lumpur 56000, Malaysia
[2]Department of Creative Product Design, Asia University, Taichung 41354, Taiwan

(Received May 11, 2026; accepted June 26, 2026)

Keywords: virtual reality, physical exhibition, spatial perception, cognitive load, immersion evaluation, quantitative analysis, experimental comparison

The perceptual and cognitive equivalence between a physical woodblock print exhibition and its immersive virtual reality (VR) reconstruction is examined in this study. A cross-over experiment with 52 participants was conducted to compare spatial fidelity, lighting realism, material authenticity, immersion, and cognitive workload across modalities. Physical exhibition parameters were captured by laser scanning, optical profilometry, spectrophotometry, and lux metering, then translated into a computer-aided design-based digital twin. The VR exhibition validation included geometric deviation analysis, tracking accuracy, latency decomposition, and colorimetric fidelity. The results indicated that spatial perception was preserved, with no significant differences between physical and VR exhibitions. Lighting realism and material authenticity were rated higher in the physical exhibition, reflecting the limitations of current rendering pipelines in reproducing micro-shadow diffusion and complex surface reflectance. Conversely, immersion was significantly enhanced when using VR, supported by six-degrees-of-freedom navigation and low-latency sensor feedback. The National Aeronautics and Space Administration–Task Load Index scores revealed moderately higher cognitive workload in VR, attributable to sensorimotor adaptation and interface demands, although remaining within acceptable limits. The results of this study show a structured trade-off: physical exhibitions excel in material and optical realism, whereas VR enhances immersion and spatial agency. The study results underscore the role of sensor technologies in bridging perceptual fidelity and provide actionable directions for advancing digital twin pipelines in cultural heritage preservation.

1. Introduction

Physical art exhibitions provide veridical spatial cues, authentic material presence, and direct light–surface interactions, whereas immersive virtual reality (VR) exhibitions offer flexible

*Corresponding author: e-mail: e-mail: hhlin@asia.edu.tw
https://doi.org/10.18494/SAM6406

ISSN 0914-4935
https://myukk.org/

spatial manipulation, dynamic scaling, and interactive exploration. Although VR systems are increasingly adopted in art exhibitions, systematic and quantitative comparisons between physical and digital modalities remain scarce.[1,2] Traditionally, artworks such as oil paintings and woodblock prints are displayed in galleries to communicate with visitors. Specifically, the aesthetic comprehension of woodblock prints (artworks created using a traditional relief printmaking technique where text, images, or patterns are carved into a block of wood) requires subtle relief variations, specular highlights, and lighting-dependent appearance changes.[3]

The proliferation of immersive VR systems enables cultural institutions to provide visitors with sensor-driven digital environments, enabling interactive spatial exploration, bypassing the physical conservation constraints inherent in traditional exhibitions. Previous studies on VR artwork exhibitions presented qualitative experience reports or platform design principles as results, presenting limitations in proposing reproducible, sensor-technology-based evaluation frameworks for VR artwork exhibitions.[4] Such frameworks must be evaluated for perception accuracy, material surface metrology, and human-factor sensor metrics in controlled experimental designs. The evaluation of the frameworks requires sensor technology to convert real-world exhibition conditions into digital engines, ensuring fidelity in immersive reconstructions.[5,6]

Immersive experiences are obtained on the basis of the psychological sensation of being there in a mediated environment. Illusion and plausibility are determined by whether users respond behaviorally and emotionally as if virtual events were real.[7,8] Because exhibition experiences are spatial and involve navigation and artwork inspection strategies, flawless tracking stability and low-latency sensor performance are essential in VR exhibitions. However, replication fidelity is a challenge to overcome. While physical exhibitions provide natural depth cues, VR systems reconstruct the artworks and the environment where they are presented, using sensor arrays, rendering pipelines, and tracking configurations.[9] Cybersickness can distort spatial perception and presence in VR environments, introducing confounding variables into evaluation data.[10] Therefore, system-level sensor indicators, such as tracking root-mean-square error (*RMSE*), signal-to-noise ratio (*SNR*), and motion-to-photon latency, must be integrated to measure behavioral and subjective metrics in VR environments.

Other than macro-spatial tracking, material surface metrology is also critical. For example, the replications of woodblock prints require ultraprecise surface profiling sensors to capture micro-topographical roughness, ink deposition thickness, and paper grain features. Conventional digitization methods often fail to capture these micro-relief details, degrading perceived authenticity. Moreover, gallery illumination shows continuous spectral variation and environmental bounce light that are computationally demanding to simulate. Accurate environmental sensor logging, such as digital lux meters, is necessary to calibrate physically based rendering in VR environments.[11]

The cognitive cost of interacting with sensor-driven interfaces is also important. Cognitive load theory posits that the working memory capacity is limited, and poor system responsiveness or tracking lag induces elevated cognitive friction.[12,13] In immersive VR, cognitive load measurement is essential because virtual displays expand sensory inputs and impose new interface-learning demands. VR is regarded as a reliable environment for investigating cognitive load during navigation, with subjective and behavioral measures converging with physical exertion under controlled conditions.[14] The National Aeronautics and Space Administration–Task Load Index (NASA-TLX) is widely used to quantify workload dimensions such as mental demand, effort, and frustration.[15] The outcomes are analyzed to explore physiological and affective responses, since immersive scenarios evoke measurable variances in stress and emotional states.[16]

To address the limitations in digital surface translation and human-system verification, we developed a controlled, sensor-calibrated, dual-environment experimental framework evaluating an immersive VR reconstruction of a woodblock print exhibition. The engineering and perceptual trade-offs between physical material ontology and digital interactive systems were investigated using a within-subject cross-over design. The environmental data obtained from calibrated lux meters and laser distance arrays, and the counterbalanced virtual parameters obtained from high-resolution head-mounted displays (HMDs) and six-degrees-of-freedom (6-DOF) tracking arrays were compared to eliminate sequence, learning, and exposure biases. The developed framework links material surface characterization data with human-factor performance indicators, including spatial perception error, navigation efficiency, presence indexing, and NASA-TLX metrics. By comparing visitor experiences across physical and virtual modalities, empirical performance benchmarks can be proposed for the design of sensor arrays in VR exhibitions, providing design guidelines for hybrid exhibition systems and advanced multi-spectral rendering sensors.

2. Methodology

2.1 Physical exhibition

A physical exhibition was established in a gallery to ensure reproducibility and comparability with the immersive VR condition. Ambient illuminance was maintained between 300 and 500 lx using diffused LED track fixtures [4000 K, color rendering index (*CRI*) > 90]. Illumination uniformity was regulated within a 0.8–1.2 ratio across the display plane. The ratio is calculated as the minimum illuminance divided by the maximum illuminance in lux. This ratio is used to measure the consistency of light across the entire wall. A ratio of 1.0 presents perfectly uniform light with zero dark spots or bright glare. Lighting must be maintained between 0.8 and 1.2 to ensure that artworks are illuminated equally. This prevents participants from being distracted by uneven shadows or artificial highlights when judging the details and distances of the woodblock prints. Continuous verification was performed using a calibrated T-10A digital lux meter (Konica Minolta, Tokyo, Japan; accuracy ±2%).[17]

Viewing distance was controlled between 1.5 and 2.0 m, consistent with museum protocols. Compliance was monitored using a GLM 50-27 C laser distance meter (Robert Bosch GmbH, Germany; accuracy ±1.0 mm).[18] Architectural geometry was captured using a BLK360 3D laser scanner (Leica Geosystems, Switzerland) and a time-of-flight sensor operating at 360,000 points/s with an accuracy of 4.0 mm, producing computer-aided design (CAD)-ready point clouds for digital twin conversion.[5] Ambient conditions were stabilized at 23 ± 1 °C and 50 ±

5% relative humidity using an SHT31 thermo-hygrometer sensor array (Sensirion AG, Switzerland).[7] Acoustic noise was regulated below 40 A-weighted decibels (dBA, a metric to mimic how the human ear perceives loudness) using a calibrated condenser microphone sound level meter.

Three woodblock prints were fabricated from hand-carved hardwood matrices. The raised image segments retained an oil-based pigment ink layer, whereas the manually recessed regions remained unprinted. To ensure long-term dimensional stability and structural resilience under physical handling, the prints were pulled on cotton-based, acid-free paper with a basis weight of 300 g/m^2. Mechanical pressing pressure was exerted during the impression stage to generate localized ink deposition thickness and subtle edge embossing impressions. This structural transfer produced distinct micro-topographical variations that directly govern specular reflection, micro-shadow formation, and perceived material texture depth.

The physical parameters measured to characterize the prints included surface relief depth (μm), arithmetic average surface roughness, ink layer uniformity, the edge sharpness of carved relief boundaries, and paper fiber texture distribution. These parameters were selected because woodblock prints exhibit a highly pronounced materiality and complex surface structure. These were measured to provide vital tactile and visual perceptual indicators in physical galleries that are susceptible to spatial degradation or smoothing during digital rendering and 3D reconstruction pipelines. To quantify these micro-surface and environmental states, a metrology sensor array was deployed as follows.

- Optical profilometer (surface morphology): Micro-topographical surface profiles and three-dimensional (3D) height maps were captured across the carved edges, inked boundaries, and unprinted paper regions using a noncontact optical profiling system (ContourGT-K, Bruker, Billerica, USA) and white-light interferometry sensors. The instrument operated with a vertical resolution of 0.1 μm and a documented measurement uncertainty of ±0.2 μm. The arithmetic average roughness was computed across a randomized multi-location testing grid to quantify localized material deviation.
- Spectrophotometer (colorimetric morphology): Surface chromatic properties were recorded in the Commission Internationale de l'Éclairage (CIE) color space using a portable spectrophotometer to model how the human eye perceives light and color.[8] The sensor configuration included the standard D65 illumination matching average daylight conditions and a standard observer angle of 10°. The configuration is defined for a standard light spectrum by CIE to represent average, midday outdoor daylight with a color temperature of approximately 6500 K. Colorimetric precision was held within an uncertainty envelope of ±0.1 ΔE units to rigorously quantify chromatic fidelity across the real and virtual prints.
- Digital lux meter (photometric monitoring): Spatial and environmental luminance stability was monitored at the artwork display and participant eye-level planes using the previously noted T-10A digital lux meter.[17] A silicon photodiode sensor was used to track real-time variations to confirm that exposure remained strictly bounded within the targeted 300–500 lx conservation range.
- Environmental sensor array (atmospheric logging): Atmospheric variables were logged at 1 min intervals using the integrated SHT31 semiconductor thermo-hygrometer sensor network.[7] This continuous tracking verified that ambient thermal and moisture conditions

remained stable, preventing paper deformation, ink hygroscopic expansion, or optical refraction fluctuations during the testing blocks.

All instruments were calibrated against verified international reference standards before the experiment, and their documented measurement uncertainty bounds were fully integrated into the subsequent human-factor statistical analysis models.

2.2 VR exhibition

Fifteen woodblock prints were digitized for the VR exhibition. The prints represented diverse carving densities, line complexities, and tonal gradations to ensure variability in surface morphology and visual detail. High-resolution imaging was performed at 600–1200 dpi with 16-bit color depth under controlled D65 illumination. Polarized lighting was employed to suppress specular reflection and preserve accurate surface characteristics. From this imaging workflow, several digital maps were generated, including an albedo (color) map, a normal map representing surface orientation, a height map reconstructing relief depth, and an ambient occlusion map. Height information was derived directly from profilometer surface data and subsequently converted into grayscale displacement maps for integration into VR rendering pipelines.

The immersive VR system was designed to replicate the physical exhibition environment with high fidelity. HMD has a resolution of 2160 × 2160 pixels per eye, operates at a refresh rate of 90 Hz, and has a field of view of 110°. Real-time motion tracking was achieved using a hybrid optical–inertial 6-DOF system that integrated infrared cameras with MEMS inertial measurement units. *RMSE* was calculated to confirm that the mean tracking error remained below 2.1 mm, ensuring accurate spatial alignment.

System responsiveness was evaluated through motion-to-photon latency decomposition. Tracking sensors introduced a delay of 4.2 ms, rendering pipelines required 11.3 ms, and display hardware contributed 3.8 ms. The total latency was 19.3 ms, which remained below the 20 ms threshold to minimize cybersickness and perceptual distortion. Geometric fidelity was validated by comparing inter-object distances between physical and virtual layouts, with the average geometric consistency error maintained lower than 1.5%. Signal quality was assessed using the *SNR* of tracking telemetry, which averaged 32.4 dB, confirming stable locomotion without disorienting jitter.

Material fidelity in the VR condition was validated by comparing several parameters with their physical counterparts. These included color differences between physical and VR displays, the consistency of relief depth rendering, and the preservation of line sharpness. Displacement scaling was calibrated using the following equation:

$$H_{VR} = k \cdot H_{measured}. \tag{1}$$

Here, H_{VR} represents the rendered displacement height in VR, $H_{measured}$ is the profilometer-derived physical measurement, and k is the perceptual scaling factor applied to ensure equivalence between modalities. Figure 1 shows the experimental setting of the physical and VR exhibitions. Room dimensions, artwork placement at a standardized center height, and corridor

(a) (b)

Fig. 1. (Color online) (a) Layout of physical woodblock print exhibition and (b) VR exhibition.

width were measured using calibrated laser scanning instruments and converted into a CAD-based 3D model. The average geometric consistency error between the physical and virtual environments was maintained lower than 2%, ensuring spatial fidelity and consistency for subsequent perceptual evaluation.[19]

2.3 Spatial perceptual and cognitive evaluations

For spatial perceptual and cognitive evaluations between the physical and VR exhibitions, a controlled experiment was conducted. Fifty-two university students (young adults aged 19–25 years old) who enrolled in the digital media arts and vocational engineering programs at University College Sedaya International in Kuala Lumpur, Malaysia, were selected as the participants to control for age-related variances in visual acuity, spatial processing, and digital interface familiarity, removing system-level rendering variables. The participants were selected to ensure basic visual acuity, spatial orientation skills, and familiarity with digital design principles, to assess architectural layout and microsurface fidelity. Before the experiment, a 5 min instruction session was provided. For the physical exhibition, the spatial boundaries and viewing distances were explained, and for the VR exhibition, an interactive calibration was conducted for all participants to adapt to the HMD optics, calibrate interpersonal interpupillary distance, and practice 6-DOF controller movements to mitigate initial sensorimotor shock, sequence bias, fatigue, and learning effects in the participants.

Perceptual evaluation was conducted using a structured questionnaire adapted from validated presence and environment appraisal scales.[20] Each dimension was measured on a 7-point Likert scale (1 = strongly disagree, 7 = strongly agree). Spatial perception was assessed for perceived room scale, artwork spacing, and layout consistency, and lighting realism was evaluated for light diffusion, glare zones, and wall-washing illumination gradients. Material authenticity was measured for the perceived realism of woodblock specimens, including paper roughness, ink layer thickness, and microshadow formation. Immersion was assessed for the subjective sense of spatial presence, suspension, and interaction agency. The internal consistency of the survey was assessed using Cronbach's alpha.[21]

The questionnaire was created by selecting and adapting validated evaluation items from the Witmer–Singer Presence Questionnaire and standard architectural appraisal indices.[22] In the questionnaire, four perceptual dimensions (spatial perception, lighting realism, material authenticity, and immersion) were selected on the basis of the technical priorities of digital twin rendering and material metrology workflows.[23] Reliability analyses were conducted for the questionnaire survey. The results of the questionnaire survey were highly reliabile (Table 1). Material authenticity showed high reliability, confirming stable participant responses regarding surface realism and depth cues. As all dimensions exceeded the 0.70 threshold, composite mean scores were appropriate for parametric analysis.[24]

Cognitive workload was assessed using NASATLX.[25] This tool was used to estimate workload across six subscales, each scored on a 0–100 scale. These subscales are used to estimate sensorimotor friction, such as adaptation to the 6DOF controller, visual fatigue from the vergence–accommodation conflict, and cognitive strain from tracking latency.[26] Raw scores were aggregated into a global workload index ranging from 0 to 100 for each condition.

- Mental demand: Required cognitive effort (thinking, deciding, and searching)
- Physical demand: Required physical effort (walking, head turning, and controller use)
- Temporal demand: Perceived time pressure
- Performance: Self-evaluation of task success and satisfaction
- Effort: Overall mental and physical exertion
- Frustration level: Experienced irritation, stress, or annoyance

Following data collection, scores were used for hypothesis testing.[27] Descriptive statistics were calculated for each perceptual dimension and NASATLX workload index.

3. Results

3.1 Physical exhibition

The surface characterization results of the fifteen woodblock prints are shown in Table 2. Relief depth, surface roughness, and colormetric morphology were measured under controlled illumination (300–500 lx). The relief depth averaged 42.6 µm [standard deviation (*SD*) = 6.8 ± 0.31 µm], confirming the presence of pronounced micro-relief features, which are typical for traditional woodblock carving. The surface roughness was 3.84 µm (*SD* = 0.72 ± 0.28 µm), reflecting localized irregularities in ink deposition and paper fiber embossing. Chromatic deviation was 1.42 (*SD* = 0.35 ± 0.15), indicating high color uniformity under D65 illumination.

Table 1
Cronbach's alpha coefficients for perceptual survey dimensions.

Dimension	Physical exhibition	VR exhibition	Threshold
Spatial perception	0.87	0.89	>0.70
Lighting realism	0.85	0.88	
Material authenticity	0.91	0.9	
Immersion	0.83	0.92	

Table 2
Surface measurement results of physical woodblock prints under controlled exhibition conditions.

Category	Parameter	*Mean*	*SD*	Uncertainty or tolerance
Material metrology	Relief depth	42.6	6.8	±0.31 μm
	Surface roughness	3.84	0.72	±0.28 μm
	Color difference	1.42	0.35	±15 units
Photometric metrology	Ambient illuminance	412	18	±2%
	Illuminance uniformity ratio	0.91	0.04	±2%
Atmospheric metrology	Ambient temperature	23.1	0.4	±0.2°C
	Relative humidity	49.7	1.8	±2.0%
Acoustic metrology	Acoustic noise level	36.4	1.2	±1.5 dBA

Illuminance at the artwork plane was 412 lx (*SD* = 18 ± 2%), confirming stable lighting conditions across the gallery.

Noncontact optical profilometry conducted across a randomized multi-location grid confirmed that the mechanical pressing process successfully generated distinctive micro-topographical variations on the paper substrates. The prints exhibited a mean relief depth of 42.6 μm (*SD* = 6.8 μm ± 0.31 μm), providing the physical boundaries necessary for localized micro-shadow formation under varyious illumination angles. The arithmetic average surface roughness was stabilized at a mean of 3.84 μm (*SD* = 0.72 ± 0.28 μm). This texture is characteristic of the complex fiber distribution in cotton-based, acid-free 300 g/m² paper and represents the authentic tactile irregularities of traditional woodblock prints. Colorimetric evaluations performed with a portable spectrophotometer under a standard D65 illumination spectrum established a stable baseline in the CIE color space. The mean spatial color variance across identical inked regions among the three fabricated prints was controlled at 1.42 (*SD* = 0.35 ± 0.15). This result indicates strong material consistency during fabrication, while preserving minor natural micro-structural irregularities that serve as an authentic test bed for perceptual evaluation tasks.

Photometric monitoring at the artwork display plane and participant eye level showed that the diffused LED lighting system maintained stable exposure throughout the testing timeline. The mean ambient illuminance was 412 lx (*SD* = 18 lx, ± 2%), securely within the targeted 300–500 lx for museum conservation. The spatial distribution of light was homogeneous, with an illuminance uniformity ratio of 0.91 (*SD* = 0.04). Because a ratio of 1.0 represents a perfectly flat lighting plane, this near-uniform profile validated that participants were insulated from artificial glare zones or deep peripheral shadows during distance estimation and detail perception tasks.

Continuous data streaming from the integrated SHT31 semiconductor thermo-hygrometer network showed that atmospheric conditions were effectively stabilized. Ambient temperature averaged 23.1 °C (*SD* = 0.4 °C), whereas relative humidity was regulated at 49.7% (*SD* = 1.8%). Stable parameters ensured that no paper warping, hygroscopic expansion of organic ink layers, or localized optical refraction shifts occurred during evaluation blocks.

Acoustic monitoring using a calibrated condenser microphone sound level meter showed that background noise was suppressed to a mean of 36.4 dBA (*SD* = 1.2 dBA). This value was maintained below the regulatory ceiling of 40 dBA, ensuring that external auditory interference did not confound cognitive load metrics during participant testing.

3.2 VR exhibition

The VR exhibition system was evaluated, focusing on tracking accuracy, geometric fidelity, signal stability, latency performance, and texture reproduction accuracy. These metrics were used for perceptual, behavioral, and cognitive comparisons between the physical and VR exhibitions to minimize human-system errors.

The hardware tracking system and rendering method were adopted for continuous monitoring to evaluate real-time performance limits. Based on *RMSE*, the hybrid optical-inertial 6-DOF sensor network maintained a mean positioning tracking error of 2.08 mm (*SD* = 0.12), maintaining it below the hardware target ceiling of 2.1 mm. This indicates stable position and orientation estimation during user locomotion. The tracking precision was calculated by *SNR* telemetry analysis, which demonstrated an average tracking signal power of 32.4 dB (*SD* = 1.4 dB). The absence of low-frequency sensor drift or high-frequency positional jitter confirms that the head tracking data fed into the virtual camera matrix remained smooth and highly stable. System responsiveness was validated by measuring the real-time motion-to-photon latency. In the VR exhibition, the time lag is unavoidable. Therefore, viewers' behavior and cognitive load scores were affected by the artwork, not by a laggy or nauseating headset experience. The cumulative total latency of 19.3 ms, comprising latency in tracking (4.2 ms), rendering (11.3 ms), and display (3.8 ms), remained securely under the 20 ms threshold, which was required to suppress vestibular-visual conflicts. Consequently, the tracking loop was sufficiently fast to eliminate sensorimotor friction, ensuring the human-factor evaluation data from tracking lag artifacts or unmitigated cybersickness symptoms.

Figure 2 shows the VR exhibition modeling workflow and system validation process. The process was used to apply the parameters to a digital twin in three stages: a development interface (CAD-based modeling workflow) for spatial data acquisition and 3D reconstruction ensured dimensional fidelity; an immersive VR gallery (spatial recreation and verification) to reflect room dimensions (18–20 m length and 6–7 m width) was replicated with geometric deviation maintained lower than 1.5%; close-up VR rendering (material surface interaction) for micro-topography displacement mapping and multi-map texture integration achieved perceptual depth fidelity, with a colormetric error lower than 3.0. The technical operations and validation thresholds applied to the workflow layer are described in Table 3.

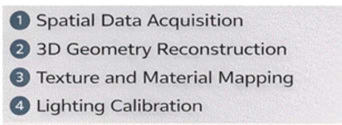

(a)

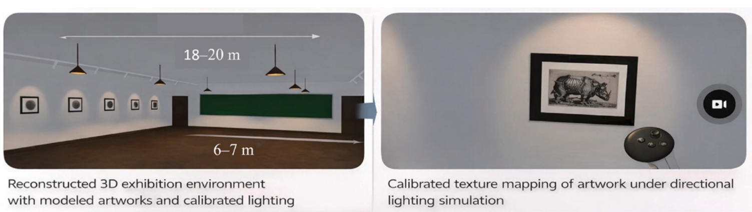

(b)

Fig. 2. (Color online) Integrated VR exhibition modeling workflow and system validation. (a) CAD-based modeling workflow. (b) VR exhibition (left) and VR rendering of print.

Table 3
VR exhibition modeling and validation workflow.

Process	Operating sensor	Validation outcome or threshold
Data acquisition	Leica BLK360 3D laser scanning; point-cloud coordinate mapping	Room geometry reference dataset (18–20 × 6–7 × 2.8–3.0 m)
3D geometry reconstruction	CAD structural modeling; strict wall, floor, and ceiling alignment	3D high-fidelity structural model skeleton; uniform artwork center line of 1.5 m
Texture and material mapping	Multi-map digitization (600–1200 dpi, 16-bit); albedo, normal, height, and ambient occlusion map injection	Scaled, micro-topographical surface textures derived from physical profilometer values
Lighting calibration	Digital lux meter matching (*mean* = 412 lx); virtual physically-based rendering (PBR) light profile generation	Calibrated illumination engine; uniform wall-washing simulation (uniformity ratio of 0.8–1.2)
Spatial recreation	Complete asset assembly within the real-time graphics rendering engine	Untethered, interactive immersive VR gallery space operating at a stable refresh rate of 90 Hz
Geometry fidelity validation	Spatial matrix cross-comparison using laser distance meters and virtual engine telemetry	Geometric consistency error of 1.44, maintained under 1.5% deviation target
Material rendering	PBR micro-relief shading; localized displacement scaling (HVR)	Perceptual material depth optimization; colorimetric discrepancy limit of < 3.0
Interaction integration	6-DOF tracking link, interactive navigation loops, user telemetry logs	Smooth real-time locomotion; mean tracking *RMSE* = 2.08 mm, motion-to-photon latency = 19.3 ms

Figure 3 shows the physical exhibition and its VR digital twin. The figure shows the execution of the cross-over experimental framework, enabling the controlled observation of behavioral and visual responses under identical spatial configurations. The physical exhibition features woodblock prints mounted along a linear wall under diffused LED track lighting (4000 K, *CRI* > 90). Measurements from the T10A digital lux meter confirmed stable ambient illuminance at 412 lx with a uniformity ratio of 0.91, ensuring consistent exposure across the viewing plane. This configuration preserves authentic light–surface interactions, microshadow gradients, and specular reflections from the ink layers—providing the tactile and visual cues essential for spatial judgment. The digital twin, rendered within HMD, was constructed using Leica BLK360 laserscan point clouds. The VR exhibition replicates the physical one (18–20 m × 6–7 m) and artwork alignment heights. Physically based rendering (PBR) techniques calibrated to the measured photometrics were used to reproduce the uniform wallwashing light profile. The geometric consistency error was maintained at 1.44 %, confirming accurate scale tracking across the virtual display plane.

Viewing distance was controlled between 1.5 and 2.0 m, corresponding to a horizontal visual angle of 25–35°, ensuring equivalent field-of-view coverage in both modalities. Figure 3(c) shows natural head orientation and binocular focus typical of unconstrained exploration. Figure 3 shows the comparison of perceptual alignment between physical and VR exhibitions, which shows the limits of digital reconstruction. High-resolution multi-map imaging (600–1200 dpi) combined with hybrid 6DOF tracking (*RMSE* = 2.08 mm) ensured macrospatial equivalence, suppressing orientation lag and spatial confusion during navigation. However, fine-scale visual differences remain. In the physical exhibition, the interaction between real illumination and paper microtopography (3.84 μm) shows dynamic microshadowing that responds instantly to

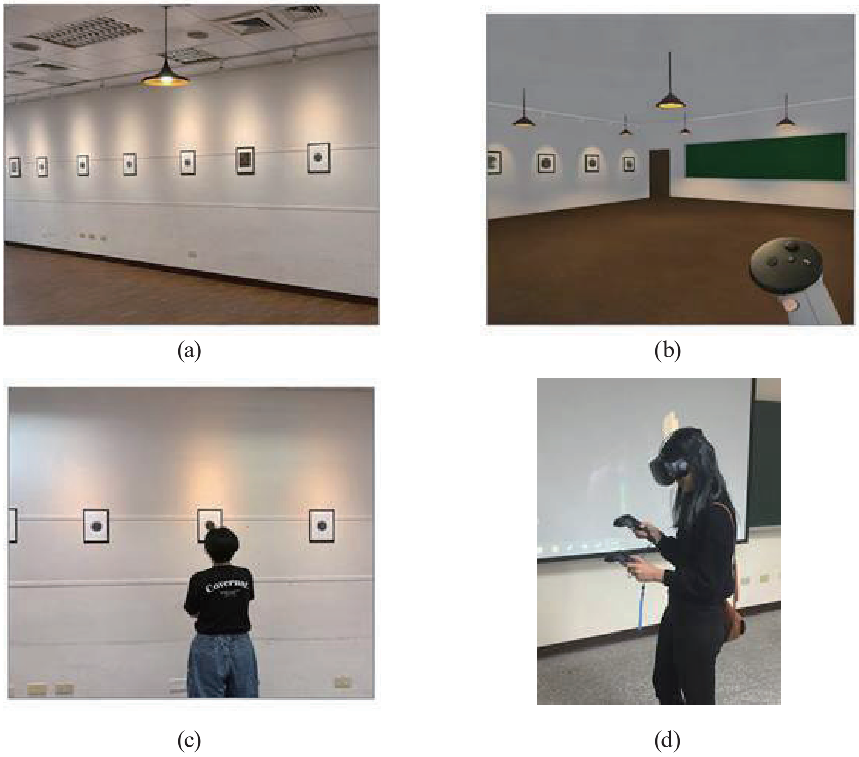

Fig. 3. (Color online) Comparative visualization of physical and immersive VR exhibition environments. (a) Physical gallery under calibrated LED illumination, (b) CAD-based VR reconstruction with verified geometric fidelity, (c) participant observing at controlled viewing distance, and (d) participant wearing HMD.

subtle changes in eye level. The VR exhibition, although calibrated using H_{VR}, introduces minor smoothing artifacts at acute viewing angles owing to pixel shading constraints. These discrepancies are used to establish an empirical baseline to analyze distance estimation error and cognitive workload across physical and digital exhibition modalities.

4. Discussion

Psychometric evaluation results show that VR successfully approximates the macro-level layout of the physical exhibition (Fig. 3). The mean spatial perception scores for the physical and VR exhibitions were 5.82 (*SD* = 0.71) and 5.64 (*SD* = 0.76), respectively (Table 4). This lack of divergence stems from the deployment of the Leica BLK360 laser scanning array during spatial acquisition. By capturing dense structural point clouds and converting them into CAD-based grids, the modeling pipeline preserved space geometry, ceiling-to-floor ratios, and frame spacing. These results show that high-density terrestrial laser scanning combined with real-time 6-DOF tracking suppresses human distance estimation errors in immersive environments.[28] The small effect size indicates that the geometric consistency error is constrained to 1.44% in the VR exhibition using the same heuristics as in the physical exhibition. Sensor-driven spatial data capture is used to support cross-over behavioral research.

Table 4
Evaluation results of physical and VR exhibitions.

Dimension	Physical exhibition	VR exhibition	*p*-value
Spatial perception	5.82	5.64	0.16
Lighting realism	5.91	5.33	0.002
Material authenticity	6.12	5.01	<0.001
Immersion	4.98	6.02	<0.001
NASA-TLX	34.2	41.8	0.003

Material authenticity revealed the largest perceptual gap. Realism scores decreased from 6.12 (physical exhibition) to 5.01 (VR exhibition), showing the strongest size effect. In terms of materials science, this difference shows the boundaries of current displacement mapping methods.[29] Although high-resolution optical scanning (600–1200 dpi) and profilometry captured paper grain roughness (3.84 μm) and ink height, variable micro-surface features are not reproduced by rendering engines. The VR exhibition lacks the following:

- Micro-shadow diffusion: Physical light scatters across fibrous paper, producing subtle shadows that shift with head movement.
- Multi-angle reflectance variation: Woodblock inks exhibit a bidirectional reflectance distribution function, generating localized specular glints that uniform shaders cannot replicate.[30]
- Active binocular depth: At micro-distances (<0.5 m), stereoscopic vision detects relief variances, whereas HMD panels flatten these onto a pixel plane.

Whereas sensors capture micro-surface data with precision, rendering methods remain the bottleneck, reducing material authenticity to approximation. Lighting was also better at the physical exhibition than at the VR exhibition. Despite calibrated lux-matched rendering (a 412 lx average and a 0.91 uniformity ratio), VR could not replicate the full optical depth of real illumination. Physical lighting involves continuous spectral distributions and multi-bounce inter-reflections.[31] PBR shaders approximated direct illumination, but failed to reproduce low-frequency gradients anchoring frames to walls. This indicates the need for high-dynamic-range radiance sensors and real-time ray-tracing architectures capable of computing global illumination profiles.

Immersion was the single dimension where VR outperformed physical exhibitions. As shown in Fig. 4, immersion scores increased from 4.98 in the VR exhibition to 6.02 in the physical exhibition. This improvement indicates the role of real-time sensor loops in heightening engagement. By maintaining ultralow motion-to-photon latency (19.3 ms), which is lower than the 20 ms threshold, the HMD delivered seamless sensorimotor feedback. Head tilts were processed within 4.2 ms (tracking loop) and displayed within 3.8 ms (panel response), creating strong spatial agency.[32] The ability to dynamically adjust perspective compensates for reduced material fidelity, enhancing psychological presence.

NASA-TLX workload indices were higher in the VR exhibition (41.8 ± 6.2) than in the physical exhibition (34.2 ± 5.1). This increase reflects the following sensory friction inherent to wearable displays:

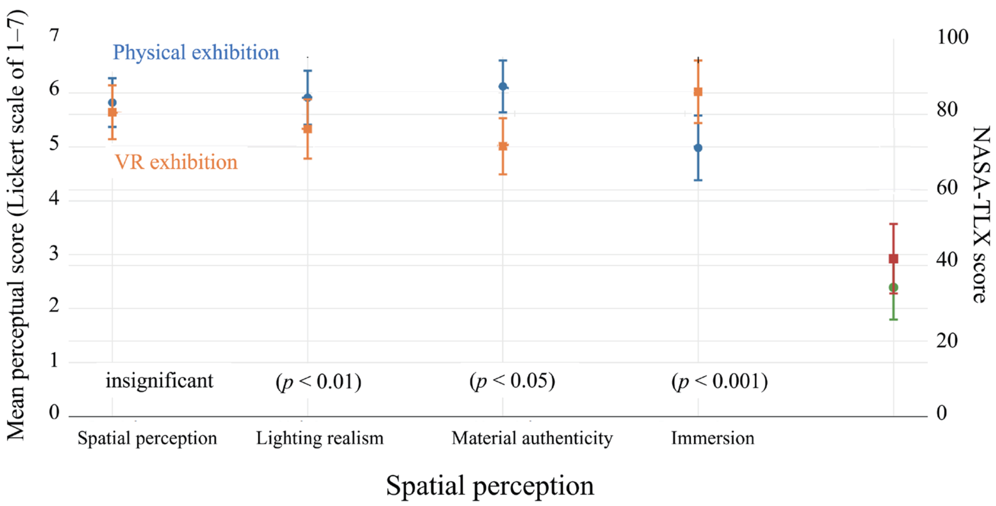

Fig. 4. (Color online) Perceptual and cognitive evaluation results between physical and VR exhibitions (red bar on right side of graph: NASA-TLX score range of physical exhibition; green bar: NASA-TLX score range of VR exhibition).

- interface adaptation for translating natural walking into controller-mediated inputs,
- convergence–accommodation conflict caused by eyes focused on fixed lenses while processing stereoscopic depth, causing minor fatigue,[33] and
- sensorimotor recalibration for adjusting to subtle tracking errors ($RMSE$ = 2.08 mm) and lens-edge distortions.

Although workload increased, scores remained moderate, indicating that low-latency design successfully limited fatigue. Such results highlight the need for continued sensor refinement to reduce cognitive strain. In the VR exhibition, bi-directional sensor optimization must be conducted, and human perceptual metrics, such as spatial scores and NASATLX indices, must be used to enhance sensor accuracy. For instance, the absence of spatial divergence prevents unnecessary hardware overspecification since a scanner precision of ±2 mm is sufficient for human spatial mapping. Real-time micro-topography shaders must be developed to address the significant decrease in material authenticity, incorporating anisotropic bidirectional reflectance distribution function models that decrease profilometer-derived roughness and scale with headtracking data. Similarly, photometric capture arrays must be upgraded, as single-point lux meters cannot capture the spectral complexity of real environments. Therefore, sensor-driven luminance matrices are required to track spectral variance across entire surfaces.

The demographics of the participants present a limitation for generalization. The participant pool was limited to a homogeneous young adult group to eliminate age-associated degradation in spatial orientation, cognitive resilience, and digital adaptability as confounding factors. Age changes how people see depth, slows down basic thinking, and makes them more prone to eye strain.[34,35] Therefore, age is an important limitation in the experiment of this study. For example, older adults adjust differently when dealing with delays in tracking systems, so the moderate NASA-TLX scores observed in this study might not apply evenly across all age groups.[34,36] This indicates that advanced rendering systems and fast tracking technology for people of all ages must be applied to confirm the digital twin's universal applicability.

5. Conclusions

A sensor-calibrated comparison between a physical art exhibition and its VR digital twin was conducted using a cross-over design. By integrating hardware-level sensor parameters with psychometric evaluation tools, a virtual museum assessment was conducted. The results show a polarization between macro-spatial fidelity and micro-surface material translation. The use of high-density laser scanning ensured that the digital architecture was insulated from structural distortion. The geometric consistency error of 1.44% occurred, preventing significant divergence in spatial perception scores, confirming that spatial equivalence between the physical and VR exhibitions was successfully maintained. Material authenticity degraded substantially, with perceptual ratings decreasing from 6.12 in the physical exhibition to 5.01 in the VR exhibition. Optical profilometry showed that the prints exhibited pronounced tactile materiality, including an average ink relief depth of 42.6 μm and a fiber roughness profile of 3.84 μm, features that current displacement shaders fail to replicate. Lighting realism diverged between modalities. Although the VR exhibition was calibrated to lux meter measurements of 412 lx mean ambient illuminance and a uniformity ratio of 0.91, the participants rated lighting realism significantly lower in VR, reflecting the absence of continuous multi-bounce inter-reflections. In contrast, immersion was significantly enhanced in VR, supported by low-latency tracking that achieved a motion-to-photon delay of 19.3 ms. This heightened engagement, however, was ensured at the cost of increased cognitive workload, with NASA-TLX scores rising from 34.2 in the physical gallery to 41.8 in VR, driven by vergence-accommodation stress and controller adaptation.

Beyond cultural heritage digitization, the results of this study can be used to provide a basis for the development of sensor and rendering systems. The absence of divergence in spatial perception indicates that a scanning precision threshold of ±2 mm is sufficient for human mapping, preventing hardware overspecification. The result on material authenticity shows a technological bottleneck, underscoring the need for multi-spectral micro-topography scanners and dynamic shading architectures that couple profilometer-derived relief data with head-tracking telemetry. The limitations of single-point lux meters imply a need for high-dynamic-range radiance sensor matrices capable of capturing full spectral and spatial complexity. NASA-TLX scores can be a quantitative benchmark for refining wearable displays, pinpointing tracking errors and latency sub-components as key sources of cognitive friction.

A sensor-driven methodology can be used to apply physical metrology to obtain human perceptual feedback. The results of this study can be used to formulate design guidelines for the development of advanced multi-spectral rendering systems, low-latency tracking arrays, and high-fidelity hybrid exhibition platforms. The results of this study confirm that VR is a complementary modality to physical exhibitions, advancing cultural heritage preservation and immersive experiential design. To widely apply the sensor-based system, further research is necessary to include people from a wider range of ages. This helps understand how the natural changes that come with aging affect the accuracy of digital twin perception.

References

1 Carrozzino and M. Bergamasco: J. Cult. Herit. **11** (2010) 452. https://doi.org/10.1016/j.culher.2010.04.001
2 S. J. Chung, S.Y. Kim, and K.H. Kim: Int. J. Hum.-Comput. Stud. **181** (2024) 103145. https://doi.org/10.1016/j.ijhcs.2023.103145
3 R. T. Azuma: Presence Teleoperators Virtual Environ. **6** (1997) 355. https://doi.org/10.1162/pres.1997.6.4.355
4 H. Xu, Y. Li, and F. Tian: Sensors **25** (2025) 4046. https://doi.org/10.3390/s25134046
5 T. Schubert, F. Friedmann, and H. Regenbrecht: Presence Teleoperators Virtual Environ. **10** (2001) 266. https://doi.org/10.1162/105474601300343603
6 J. Steuer: J. Commun. **42** (1992) 73. https://doi.org/10.1111/j.1460-2466.1992.tb00812.x
7 M. Slater: Philos. Trans. R. Soc. Lond. B Biol. Sci. **364** (2009) 3549. https://doi.org/10.1098/rstb.2009.0138
8 M. Slater, D. Banakou, A. Beacco, J. Gallego, F. Macia-Varela, and R. Oliva: Front. Virtual Real. **3** (2022) 914392. https://doi.org/10.3389/frvir.2022.914392
9 R. P. Darken and J. L. Sibert: Int. J. Hum.-Comput. Interact. **8** (1996) 49. https://doi.org/10.1080/10447319609526140
10 R. S. Kennedy, N.E. Lane, K. S. Berbaum, and M.G. Lilienthal: Int. J. Aviat. Psychol. **3** (1993) 203. https://doi.org/10.1207/s15327108ijap0303_3
11 P. Debevec: Proc. 25th Annual Conf. Computer Graphics and Interactive Techniques (ACM, 1998) 189. https://doi.org/10.1145/280814.2808
12 T. de Jong: Instr Sci **38** (2010) 105. https://doi.org/10.1007/s11251-009-9110-0
13 J. Sweller: Cogn. Sci. **12** (1988) 257. https://doi.org/10.1207/s15516709cog1202_4
14 B. Mostefai, A. Balla, and P. Trigano: Cogn. Syst. Res. **56** (2019) 82. https://doi.org/10.1016/j.cogsys.2019.03.006
15 H. R. Jex: Adv. Psychol. **52** (1988) 5. https://doi.org/10.1016/S0166-4115(08)62381-X
16 C. Crescentini, L. Chittaro, V. Capurso, R. Sioni, and F. Fabbro: Comput. Hum. Behav. **59** (2016) 304. https://doi.org/10.1016/j.chb.2016.02.031
17 P. Milgram and F. Kishino: IEICE Trans. Inf. & Syst. **E77-D** (1994) 1321. https://globals.ieice.org/en_transactions/information/10.1587/e77-d_12_1321/_p
18 F. G. W. C. Paas, J. J. G. van Merriënboer, and J. J. Adam: Percept. Mot. Skills **79** (1994) 419. https://doi.org/10.2466/pms.1994.79.1.419
19 W. Li, Y. Zhang, R. Li, L. Zhang, X. Zhang, H. Li, P. Nie, and S. Zhang: Appl. Sci. **14** (2024) 3135. https://doi.org/10.3390/app14083135
20 B. G. Witmer and M. J. Singer: Presence Teleoperators Virtual Environ. **7** (1998) 225. https://doi.org/10.1162/105474698565686
21 L. J. Cronbach: Psychometrika **16** (1951) 297. https://doi.org/10.1007/BF02310555
22 J. Vasconcelos-Raposo, M. Melo, L. Barbosa, C. Teixeira, L. Cabral, and M. Bessa: Behav. Inf. Technol. **40** (2021) 1417. https://doi.org/10.1080/0144929X.2020.1754911
23 F. Ojeda de Ocampo, G. Hernández-Melgarejo, A. Ramírez-Treviño, and R.Q. Fuentes-Aguilar: Appl. Sci. **16** (2026) 3102. https://doi.org/10.3390/app16063102
24 A. Cao, K. K. Chintamani, A. K. Pandya, and R. D. Ellis: Behav. Res. Methods **41** (2009) 113. https://doi.org/10.3758/BRM.41.1.113
25 S. G. Hart and L. E. Staveland: Adv. Psychol. **52** (1988) 139. https://doi.org/10.1016/S0166-4115(08)62386-9
26 J. R. Wilson and S. Sharples: Evaluation of Human Work, 4th ed., eds. J.R. Wilson and S. Sharples (CRC Press, Boca Raton, 2015) Chap. 1. https://doi.org/10.1201/b18362
27 P. E. Shrout and J. L. Fleiss: Psychol. Bull. **86** (1979) 420. https://doi.org/10.1037//0033-2909.86.2.420
28 D. F. Laefer, L. Truong-Hong, and M. Fitzgerald: Open Constr. Build. Technol. J. **4** (2011) 16. https://doi.org/10.2174/2213275911104010016
29 P. E. Shrout and J.L. Fleiss: Psychol. Bull. **86** (1979) 420. https://doi.org/10.1037//0033-2909.86.2.420
30 K. Kehren, P. Urban, and E. Dörsam: Proc. 19th Color Imaging Conference (IS&T, 2011) 316. https://doi.org/10.2352/CIC.2011.19.1.art00060
31 G. Gonçalves, M. Melo, P. Monteiro, H. Coelho, and M. Bessa: Comput. Graph. **117** (2023) 172. https://doi.org/10.1016/j.cag.2023.10.021
32 N. Tian, P. Lopes, and R. Boulic: Virtual Real. **26** (2022) 1409. https://doi.org/10.1007/s10055-022-00638-2
33 A. Varshney, M. E. Munns, J. Kasowski, M. Zhou, C. He, S. T. Grafton, B. Giesbrecht, M. Hegarty, and M. Beyeler: Sci. Rep. **14** (2024) 5949. https://doi.org/10.1038/s41598-024-56048-8
34 A. Plechatá and V. Sahula: Front. Psychol. **10** (2019) 1330. https://doi.org/10.3389/fpsyg.2019.01330

35 A. Park, H. Kang, and S.-Y. Kim: PeerJ **14** (2026) e21169. https://doi.org/10.7717/peerj.21169
36 S. R. Anderson, C. Kirkley, A. J. Baughman, C. Cram, E. Andrews, K. J. Kim, R. DiDomenica, M. Stosic, S.T. Bell, K. Marshall-Goebel, and D. M. Buckland: Front. Psychol. **17** (2026) 1713354. https://doi.org/10.3389/fpsyg.2026.1713354

About the Authors

Ming Zhang received her bachelor's and master's degrees in Visual Arts from the Academy of Fine Arts in Lecce, Italy. She is currently pursuing a doctoral degree at the Institute of Creative Arts and Design, UCSI University, Kuala Lumpur, Malaysia. Her primary research focuses on art and design. (1650392614@qq.com).

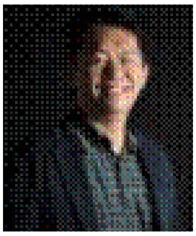

Hsin-Hung Lin is a professor at the Department of Creative Product Design of Asia University, Taichung, Taiwan. His major research interests include the application of fuzzy set theory in product design, concurrent engineering in product design, computer-aided design, the application of neural networks and gray theory in product design, color planning for product design, heat transfer analysis, and the application of reverse engineering in product design.
(hhlin@asia.edu.tw)